

COMPARATIVE ANALYSIS AND EVALUATION OF A CO₂ TRANSCRITICAL REFRIGERATION SYSTEM BEFORE AND AFTER OPTIMIZATION CONFIGURATIONS

Evangelos Syngounas^{a,b}, Dimitrios Tsimpoukis^{a,b}, Georgios Mitsopoulos^b, Sergio Girotto^c, Stavros Anagnostatos^{a,d}

^a Energy and Environmental Management Department, Head Department of Development, Metro S.A, Greece

^b Thermal Department, School of Mechanical Engineering, National Technical University of Athens, Greece

^c Enex S.r.l, Italy

^d Electric Power Department, School of Electrical Engineering, National Technical University of Athens, Greece

1. Introduction

According to F-Gas Regulation 517/2014, the use of HFC's with a GWP above 150 will be forbidden since 2022 in new multipack centralised refrigerating units for commercial use with a rated capacity higher than 40 kW, except in the primary circuit of cascade systems where refrigerants with GWP up to 1500 may be used. Due to this regulation, steps toward more environmentally friendly refrigerants are made from the representatives of the retail sector. In this context, a transcritical CO₂ system has been installed in a supermarket in the area of Pyrgos, Greece, which is in the region of Southern Europe. However, as the energy consumption of transcritical CO₂ systems is high in warmer areas, some configurations aiming in the improvement of the plant's energy efficiency have been adopted, such as a parallel compressor, adiabatic cooling in the gas cooler, and a liquid ejector block.

2. Refrigeration unit

The transcritical CO₂ refrigeration plant has installed capacity equal to 57 kW for the MT circuit, and 27 kW for the LT circuit. Figure 1 depicts the installed system of the supermarket, and in Figure 2 the P&ID of the unit is given.



Figure 1. Transcritical CO₂ unit of supermarket in Pyrgos, Greece

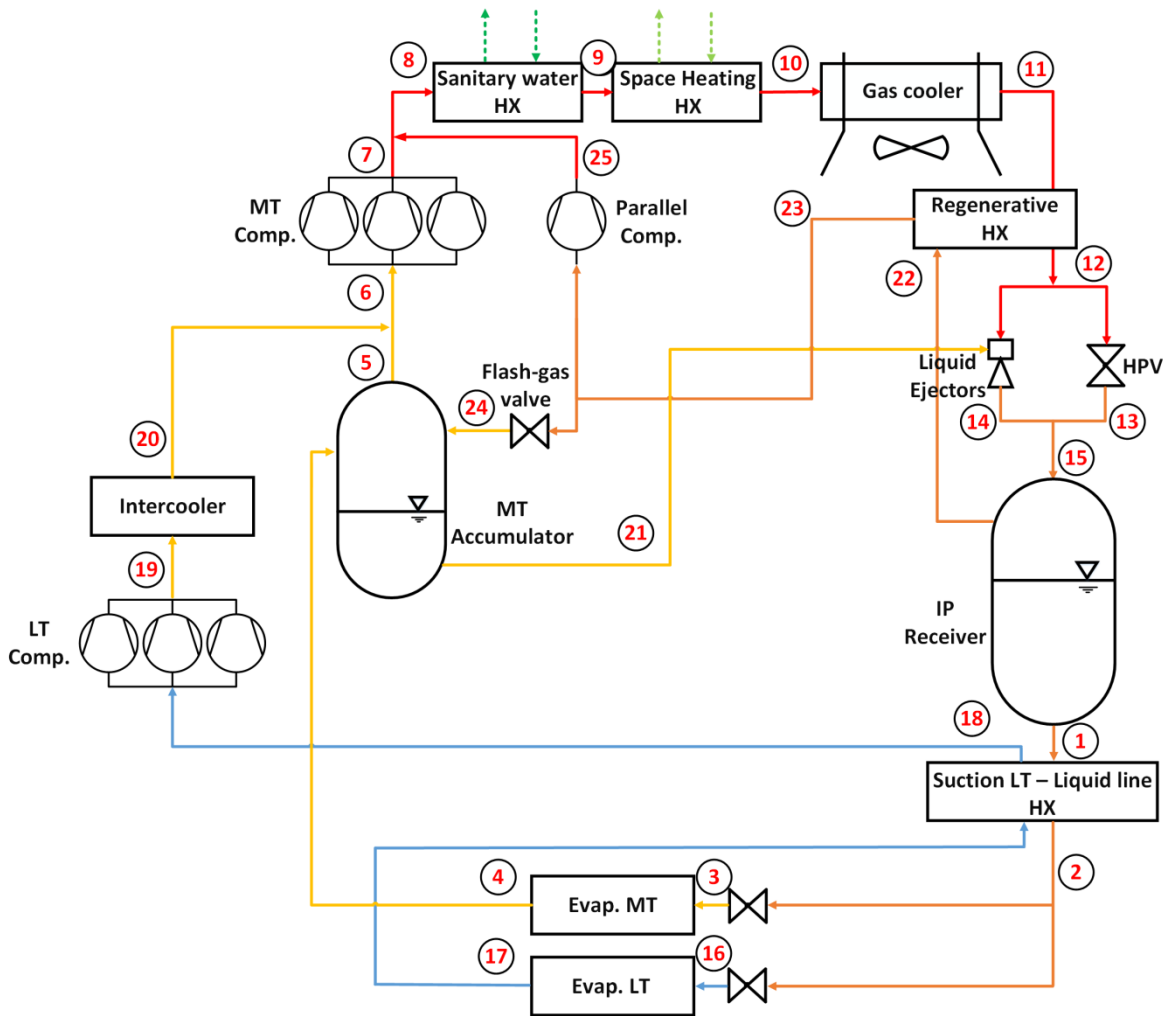


Figure 2. P&ID of CO₂ refrigeration system

When the parallel compressor is activated, it compresses the flash gas of the liquid receiver from the intermediate pressure to the high pressure of the system, which would be otherwise compressed by the MT compressors. This is a widely used measure in CO₂ transcritical systems in warm areas, since there is significant amount of flash gas during the transcritical operation of such systems. The temperature of parallel compressor's activation is set to be 23°C, since there must be a minimum amount of flash gas in the suction of the compressor.

The adiabatic cooling configuration in the gas cooler has also a very important contribution in the improvement of the plant's efficiency. When the ambient temperature exceeds 28°C, water is poured in a specially designed surface of the gas cooler, thus increasing the relative humidity of the air with a simultaneous decrease of its temperature, which tends to reach its wet bulb temperature.

The liquid ejector block is also a technology that offers important energy savings. Liquid ejectors give the opportunity of overfeeding the evaporators, using their entire area for the evaporation, as Girotto explains [1]. In this way, the superheat which is necessary to ensure clear vapour entering the compressors, can reach values near to zero and as a result the evaporation temperature of the MT evaporators can be increased, which leads

in decreased energy consumption. In practice, the refrigerant out of the MT evaporators has superheat near to 2 to 3 K, in order for the valves to be able to control their opening. Since the superheat is very low, the refrigerant in the outlet of the MT evaporators may contain liquid, which is separated from its vapour part inside the accumulator. When the liquid level of the accumulator reaches a predefined level, the liquid ejectors are activated to remove the liquid from the suction accumulator. The refrigerant which comes out of the liquid ejectors in the intermediate pressure of the system mixes with the refrigerant after the high pressure valve and it then enters in the liquid receiver.

A heat exchanger after the liquid receiver is also employed, which enables the heat transfer from the liquid line to the refrigerant after the low temperature evaporators. In this way, the necessary superheat in the suction of the LT compressors is achieved, and at the same time the liquid refrigerant before the evaporators is subcooled. This heat exchanger offers the opportunity of working with lower superheat values, enabling a certain increase of evaporation temperature of LT evaporators.

For the first months of its operation, the parallel compressor, the adiabatic cooling configuration and the liquid ejectors of the refrigeration system were not activated, so the system was working like a typical booster unit. In April, all of the aforementioned technologies were activated, and as a result the unit reached its maximum energy saving potential. The operating conditions of the system before and after the configurations are described in Table 1.

Table 1. Operating conditions of the refrigeration system

Parameter	Value before optimization	Value after optimization
MT evaporation temperature	-10.6 °C	-4.5 °C
LT evaporation temperature	-35 °C	-28.5 °C
Superheat in MT evaporators	12 °C	2.5 °C
Superheat in LT evaporators	9 °C	5 °C
$T_{gc,out}$ activating parallel compressor	-	23 °C
T_{amb} activating adiabatic cooling	-	28 °C

3. Modeling and validation of the investigated systems

The modeling of the system is based on the application of the suitable thermodynamic equations, which are presented in Figure 3.

Refrigeration loads $Q_{evap} = \dot{m} \cdot (h_{evap,out} - h_{evap,in})$ If $T_{amb} \geq 5$ and $T_{amb} \leq 30$: $LF_{MT} = \left(1 - (1 - 0.66) \cdot \left(\frac{30 - T_{amb}}{30 - 5}\right)\right)$ If $T_{amb} \geq 5$ and $T_{amb} \leq 30$: $LF_{LT} = \left(1 - (1 - 0.8) \cdot \left(\frac{30 - T_{amb}}{30 - 5}\right)\right)$ $Q_{evapMT} = LF_{MT} \cdot Q_{evapMTmax}$ $Q_{evapLT} = LF_{LT} \cdot Q_{evapLTmax}$ Efficiencies $\eta_{total} = \eta_{is} \cdot \eta_{mech}$ $\eta_{mech} = 95\%$	Compressors $W = \dot{m} \cdot \frac{h_{8,is} - h_7}{\eta_{total}}$ $h_7 = \frac{h_{7,is} - h_6}{\eta_{is}} + h_6$ Mixing points $\dot{m}_7 \cdot h_7 + \dot{m}_{25} \cdot h_{25} = \dot{m}_8 \cdot h_8$ Liquid ejectors $\dot{m}_{21} \cdot h_{21} + \dot{m}_{11} \cdot h_{12} = \dot{m}_{15} \cdot h_{15}$ Liquid receiver $\dot{m}_1 = \dot{m}_{15} \cdot (1 - x_{15})$ $\dot{m}_{22} = \dot{m}_{15} \cdot x_{15}$
-------------------------------------------------------------------------------------------------------------------------------------------------------------------------------------------------------------------------------------------------------------------------------------------------------------------------------------------------------------------------------------------------------------------------------------------------------------------------------------------------------------------------------------------------------------------	------------------------------------------------------------------------------------------------------------------------------------------------------------------------------------------------------------------------------------------------------------------------------------------------------------------------------------------------------------------------------------------------------------------------------------------------------------------------------

Figure 3. Equations used for the modeling of the system

The equations which give the refrigeration loads for the MT and LT circuits in correlation with the ambient temperature are proposed by Zhang [2]. The maximum refrigeration loads of the supermarket are lower than the installed capacity, and they are equal to 38.19 kW for MT and 18.09 kW for LT. For ambient temperatures lower than 5°C, LF_{MT} is equal to 0.66 and LF_{LT} is equal to 0.8, while for ambient temperatures greater than 30°C, both are equal to 1. The total efficiency of the compressors is calculated with Dorin Software [3].

Regarding the correlation between the ambient temperature, the gas cooler outlet temperature and the high pressure of the unit, Table 2 contains the relevant equations that are based on real measurements of the system.

Table 2. Correlations for the calculation of the gas cooler outlet temperature and the system's high pressure

Ambient Temperature Range	Gas cooler outlet Temperature [°C]	Condenser/Gas cooler outlet Pressure [bar]
$T_{amb} \leq 7.2^\circ\text{C}$	$14^\circ\text{C} - 3.2^\circ\text{C} = 10.8^\circ\text{C}$	Saturated pressure of $T_{cond} = 14^\circ\text{C}$
$7.2^\circ\text{C} < T_{amb} \leq 14^\circ\text{C}$	$T_{amb} + 6.8^\circ\text{C} - 3.2^\circ\text{C} = T_{amb} + 3.6^\circ\text{C}$	Saturated pressure of $T_{cond} = T_{amb} + 6.8^\circ\text{C}$
$14^\circ\text{C} < T_{amb} \leq 24^\circ\text{C}$	$0.9194 \cdot T_{amb} + 4.728$	$1.5493 \cdot T_{gc,out} + 36.428$
$T_{amb} > 24^\circ\text{C}$	$T_{amb} + 2.79^\circ\text{C}$	Optimized

Before the implementation of the energy saving measures, the system was operating from October 2018 to April 2019. However, the measurement setup of the power consumption of the rack was installed in December 2018. Figure 4 depicts the real energy consumption of the rack and the values that are given by the model for every week of the unit's operation.

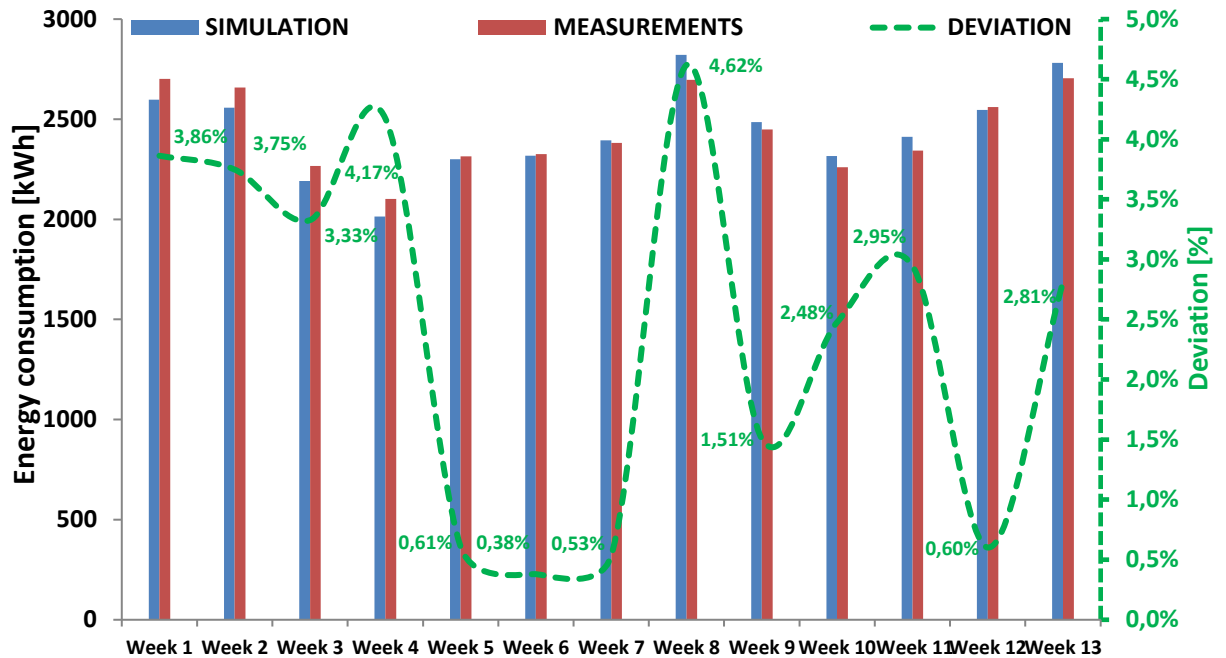


Figure 4. Validation for 13 weeks of operation before the configurations

As it can be seen, the values of the prediction model are very close to the real measurements, which means that it can be considered quite accurate. More specifically, the maximum deviation is **4.6%**, while the mean deviation of all weeks is **2.4%**. For the calculation of the energy consumption after the modifications, a similar model is also used, including the parallel compressor, the adiabatic cooling in the gas cooler and the alterations of the operating conditions, as they are described in Table 1. The temperatures that are used for the calculations are the real mean temperatures of Pyrgos for each hour of every month, from April 2018 to March 2019.

4. Results

The final results for a whole year of operation are depicted in Figure 5. Concerning the values before the optimization procedures, the energy consumption from December 2018 to April 2019 is measured, while the other months are based on the model. The model is also used for the calculation of the energy consumption after the energy saving configurations.

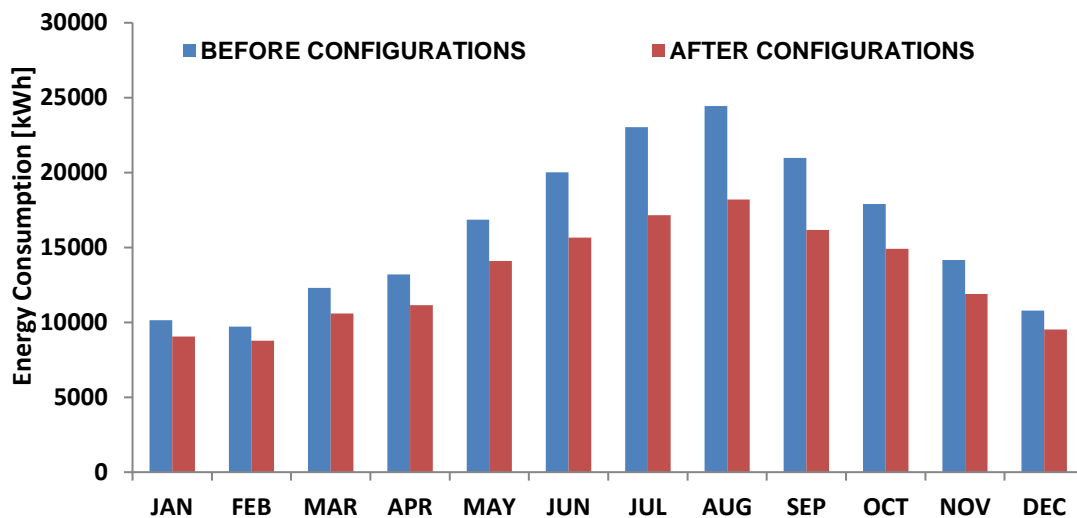


Figure 5. Monthly energy consumption before and after the configurations

Before the configurations, the system exhibits high electricity consumption during the warmer months, while during the colder months the energy consumption is similar to that of an HFC system. After the configurations, there is a small improvement during the colder months, but the significant advantage is obtained during the warmer months, as the consumption remains at very low levels compared to the situation before the configurations. For example, the consumption during January is **12.7%** lower after the configurations, while the consumption during August is **26.9%** lower. The total annual electricity consumption is calculated **193,528 kWh** for the case before the optimization actions and **154,027 kWh** after them, which means **20.4%** less energy consumption during a year, due to the fact that the energy saving configurations have been adopted.

References

- [1] S. Girotto, 2017. Improved Transcritical CO₂ refrigeration systems for warm climates. In: 7th IIR Conference: Ammonia and CO₂ Refrigeration Technologies, Ohrid.
- [2] M. Zhang, 2006. Energy analysis of various supermarket refrigeration systems. In: Proceedings of the 11th International Refrigeration and Air Conditioning Conference, 17th – 20th July; West Lafayette, USA
- [3] Dorin 2018, Dorin Software 18.07. (<http://www.dorin.com/en/Software>)